Transmission enhancement through deep subwavelength apertures using connected split ring resonators

Damla Ates,[1,*] Atilla Ozgur Cakmak,[1] Evrim Colak,[1] Rongkuo Zhao,[2,3] C. M. Soukoulis,[2,4] and Ekmel Ozbay[1,5]

[1]*Department of Electrical and Electronics Engineering, Nanotechnology Research Center (NANOTAM), Bilkent University, 06800, Ankara, Turkey*

[2]*Department of Physics and Astronomy and Ames Laboratory, Iowa State University, Ames, Iowa 50011, USA*

[3]*Applied Optics Beijing Area Major Laboratory, Department of Physics, Beijing Normal University, Beijing 100875, China*

[4]*Institute of Electronic Structure and Laser-FORTH, and Department of Materials Science and Technology, University of Crete, Greece*

[5]*Department of Physics, Bilkent University, 06800, Ankara, Turkey*

**damla@ee.bilkent.edu.tr*

Abstract: We report astonishingly high transmission enhancement factors through a subwavelength aperture at microwave frequencies by placing connected split ring resonators in the vicinity of the aperture. We carried out numerical simulations that are consistent with our experimental conclusions. We experimentally show higher than 70,000-fold extraordinary transmission through a deep subwavelength aperture with an electrical size of λ/31×λ/12 (width × length), in terms of the operational wavelength. We discuss the physical origins of the phenomenon. Our numerical results predict that even more improvements of the enhancement factors are attainable. Theoretically, the approach opens up the possibility for achieving very large enhancement factors by overcoming the physical limitations and thereby minimizes the dependence on the aperture geometries.

OCIS codes: (160.3918) Materials: Metamaterials; (050.1220) Diffraction and gratings: Aperture.

References and links

1. H. A. Bethe, "Theory of diffraction by small holes," Phys. Rev. **66**(7-8), 163–182 (1944).
2. T. W. Ebbesen, H. J. Lezec, H. F. Ghaemi, T. Thio, and P. A. Wolff, "Extraordinary optical transmission through sub-wavelength hole arrays," Nature **391**(6668), 667–669 (1998).
3. L. Martín-Moreno, F. J. García-Vidal, H. J. Lezec, K. M. Pellerin, T. Thio, J. B. Pendry, and T. W. Ebbesen, "Theory of extraordinary optical transmission through subwavelength hole arrays," Phys. Rev. Lett. **86**(6), 1114–1117 (2001).
4. J. A. Porto, F. J. Garcia-Vidal, and J. B. Pendry, "Transmission resonances on metallic gratings with very narrow slits," Phys. Rev. Lett. **83**(14), 2845–2848 (1999).
5. J. Bravo-Abad, A. Degiron, F. Przybilla, C. Genet, F. J. Garcia-Vidal, L. Martin-Moreno, and T. W. Ebbesen, "How light emerges from an illuminated array of subwavelength holes," Nat. Phys. **2**(2), 120–123 (2006).
6. K. G. Lee, and Q.-H. Park, "Coupling of surface plasmon polaritons and light in metallic nanoslits," Phys. Rev. Lett. **95**(10), 103902 (2005).
7. Y. Xie, A. R. Zakharian, J. V. Moloney, and M. Mansuripur, "Transmission of light through periodic arrays of sub-wavelength slits in metallic hosts," Opt. Express **14**(14), 6400–6413 (2006).
8. F. J. García de Abajo, J. J. Sáenz, I. Campillo, and J. S. Dolado, "Site and lattice resonances in metallic hole arrays," Opt. Express **14**(1), 7–18 (2006).
9. F. Marquier, J.-J. Greffet, S. Collin, F. Pardo, and J. L. Pelouard, "Resonant transmission through a metallic film due to coupled modes," Opt. Express **13**(1), 70–76 (2005).
10. H. F. Schouten, N. Kuzmin, G. Dubois, T. D. Visser, G. Gbur, P. F. A. Alkemade, H. Blok, G. W. Hooft, D. Lenstra, and E. R. Eliel, "Plasmon-assisted two-slit transmission: Young's experiment revisited," Phys. Rev. Lett. **94**(5), 053901 (2005).
11. A. Dogariu, T. Thio, L. J. Wang, T. W. Ebbesen, and H. J. Lezec, "Delay in light transmission through small apertures," Opt. Lett. **26**(7), 450–452 (2001).

#121693 - $15.00 USD Received 17 Dec 2009; revised 31 Jan 2010; accepted 2 Feb 2010; published 12 Feb 2010

12. Q.- Wang, J.- Li, C.- Huang, C. Zhang, and Y.-y. Zhu, "Enhanced optical transmission through metal films with rotation-symmetrical hole arrays," Appl. Phys. Lett. **87**(9), 091105 (2005).
13. W. L. Barnes, W. A. Murray, J. Dintinger, E. Devaux, and T. W. Ebbesen, "Surface plasmon polaritons and their role in the enhanced transmission of light through periodic arrays of subwavelength holes in a metal film," Phys. Rev. Lett. **92**(10), 107401 (2004).
14. K. J. K. Koerkamp, S. Enoch, F. B. Segerink, N. F. van Hulst, and L. Kuipers, "Strong influence of hole shape on extraordinary transmission through periodic arrays of subwavelength holes," Phys. Rev. Lett. **92**(18), 183901 (2004).
15. T. Matsui, A. Agrawal, A. Nahata, and Z. V. Vardeny, "Transmission resonances through aperiodic arrays of subwavelength apertures," Nature **446**(7135), 517–521 (2007).
16. H. F. Ghaemi, T. Thio, D. E. Grupp, T. W. Ebbesen, and H. J. Lezec, "Surface plasmons enhance optical transmission through subwavelength holes," Phys. Rev. B **58**(11), 6779–6782 (1998).
17. F. J. Garcia de Abajo, "Light transmission through a single cylindrical hole in a metallic film," Opt. Express **10**(25), 1475–1484 (2002).
18. A. R. Zakharian, M. Mansuripur, and J. V. Moloney, "Transmission of light through small elliptical apertures," Opt. Express **12**(12), 2631–2648 (2004).
19. F. J. García-Vidal, E. Moreno, J. A. Porto, and L. Martín-Moreno, "Transmission of light through a single rectangular hole," Phys. Rev. Lett. **95**(10), 103901 (2005).
20. L. Yin, V. K. Vlasko-Vlasov, A. Rydh, J. Pearson, U. Welp, S.-H. Chang, S. K. Gray, G. C. Schatz, D. B. Brown, and C. W. Kimball, "Surface plasmons at single nanoholes in Au films," Appl. Phys. Lett. **85**(3), 467–469 (2004).
21. A. Degiron, and T. W. Ebbesen, "Analysis of the transmission process through single apertures surrounded by periodic corrugations," Opt. Express **12**(16), 3694–3700 (2004).
22. F. J. Garcia-Vidal, L. Martin-Moreno, H. J. Lezec, and T. W. Ebbesen, "Focusing light with a single subwavelength aperture flanked by surface corrugations," Appl. Phys. Lett. **83**, 4500–4502 (2003).
23. H. Caglayan, I. Bulu, and E. Ozbay, "Plasmonic structures with extraordinary transmission and highly directional beaming properties," Microw. Opt. Technol. Lett. **48**(12), 2491–2496 (2006).
24. S. S. Akarca-Biyikli, I. Bulu, and E. Ozbay, "Enhanced transmission of microwave radiation in one-dimensional metallic gratings with subwavelength aperture," Appl. Phys. Lett. **85**(7), 1098–1100 (2004).
25. S. S. Akarca-Biyikli, I. Bulu, and E. Ozbay, "Resonant excitation of surface plasmons in one-dimensional metallic grating structures at microwave frequencies," J. Opt. Pure Appl. Opt. **7**(2), S159–S164 (2005).
26. L. Martín-Moreno, F. J. García-Vidal, H. J. Lezec, A. Degiron, and T. W. Ebbesen, "Theory of highly directional emission from a single subwavelength aperture surrounded by surface corrugations," Phys. Rev. Lett. **90**(16), 167401 (2003).
27. H. J. Lezec, A. Degiron, E. Devaux, R. A. Linke, L. Martin-Moreno, F. J. Garcia-Vidal, and T. W. Ebbesen, "Beaming light from a subwavelength aperture," Science **297**(5582), 820–822 (2002).
28. G. Gbur, H. F. Schouten, and T. D. Visser, "Achieving superresolution in near-field optical data readout systems using surface plasmons," Appl. Phys. Lett. **87**(19), 191109 (2005).
29. T. Ishi, J. Fujikata, K. Makita, T. Baba, and K. Ohashi, "Si nano-photodiode with a surface plasmon antenna," Jpn. J. Appl. Phys. **44**(12), 364–366 (2005).
30. C. Liu, V. Kamaev, and Z. V. Vardeny, "Efficiency enhancement of an organic light-emitting diode with a cathode forming two-dimensional periodic hole array," Appl. Phys. Lett. **86**(14), 143501 (2005).
31. X. Luo, and T. Ishihara, "Sub-100-nm photolithography based on plasmon resonance," Jpn. J. Appl. Phys. **43**(No. 6B), 4017–4021 (2004).
32. D. B. Shao, and S. C. Chen, "Surface-plasmon-assisted nanoscale photolithography by polarized light," Appl. Phys. Lett. **86**(25), 253107 (2005).
33. P. R. H. Stark, A. E. Halleck, and D. N. Larson, "Short order nanohole arrays in metals for highly sensitive probing of local indices of refraction as the basis for a highly multiplexed biosensor technology," Methods **37**(1), 37–47 (2005).
34. S. M. Williams, K. R. Rodriguez, S. Teeters-Kennedy, S. Shah, T. M. Rogers, A. D. Stafford, and J. V. Coe, "Scaffolding for nanotechnology: extraordinary infrared transmission of metal microarrays for stacked sensors and surface spectroscopy," Nanotechnology **15**(10), S495–S503 (2004).
35. H. Rigneault, J. Capoulade, J. Dintinger, J. Wenger, N. Bonod, E. Popov, T. W. Ebbesen, and P.-F. Lenne, "Enhancement of single-molecule fluorescence detection in subwavelength apertures," Phys. Rev. Lett. **95**(11), 117401 (2005).
36. J. B. Pendry, L. Martín-Moreno, and F. J. Garcia-Vidal, "Mimicking surface plasmons with structured surfaces," Science **305**(5685), 847–848 (2004).
37. F. J. Garcia-Vidal, L. Martin-Moreno, and J. B. Pendry, "Surfaces with holes in them: new plasmonic metamaterials," J. Opt. Pure Appl. Opt. **7**(2), S97–S101 (2005).
38. N. Katsarakis, M. Kafesaki, I. Tsiapa, E. N. Economou, and C. M. Soukoulis, "High transmittance left-handed materials involving symmetric split-ring resonators," Photon. Nanostructures **5**(4), 149–155 (2007).
39. A. Alu, F. Bilotti, N. Engheta, and L. Vegni, "Metamaterial covers over a small aperture," IEEE Trans. Antenn. Propag. **54**(6), 1632–1643 (2006).
40. R. Marques, F. Mesa, J. Martel, and F. Medina, "Comparative analysis of edge- and broadside- coupled split ring resonators for metamaterial design-theory and experiments," IEEE Trans. Antenn. Propag. **51**(10), 2572–2581 (2003).
41. K. Aydin, A. O. Cakmak, L. Sahin, Z. Li, F. Bilotti, L. Vegni, and E. Ozbay, "Split-ring-resonator-coupled enhanced transmission through a single subwavelength aperture," Phys. Rev. Lett. **102**(1), 013904 (2009).

#121693 - $15.00 USD Received 17 Dec 2009; revised 31 Jan 2010; accepted 2 Feb 2010; published 12 Feb 2010

42. A. O. Cakmak, K. Aydin, E. Colak, Z. Li, F. Bilotti, L. Vegni, and E. Ozbay, "Enhanced transmission through a subwavelength aperture using metamaterials," Appl. Phys. Lett. **95**(5), 052103 (2009).
43. K. B. Alici, F. Bilotti, L. Vegni, and E. Ozbay, "Optimization and tunability of deep subwavelength resonators for metamaterial applications: complete enhanced transmission through a subwavelength aperture," Opt. Express **17**(8), 5933–5943 (2009).
44. F. Bilotti, L. Scorrano, E. Ozbay, and L. Vegni, "Enhanced transmission through a sub-wavelength aperture: resonant approaches employing metamaterials," J. Opt. Pure Appl. Opt. **11**(11), 114029 (2009).

1. Introduction

Only a small portion of an incident beam is allowed to pass through a tiny hole in an opaque screen. This phenomenon was electromagnetically explained in the last century by Bethe [1]. He showed that the transmission efficiency of such a hole would be proportional to $(r/\lambda)^4$. Here, r represented the radius of the hole and λ corresponded to the operational wavelength of the electromagnetic signal. His theories were based on an idealized two dimensional diffraction model of an infinitesimally thin screen. In accordance with Bethe's predictions, electromagnetic wave transmission through subwavelength holes remained a challenging topic until the first proposals of Ebbesen *et al*. [2]. Extraordinary transmission phenomenon through an array of subwavelength holes milled in an opaque metal screen was first demonstrated with the aid of the surface plasmons. Several orders of magnitude more transmission than Bethe's calculations was observed owing to the resonant interactions of the incident photons with the surface plasmon polaritons of the metal surface. This study has gained an increasing attention and has encouraged the researchers to seek brand new transmission enhancement results through subwavelength apertures. Extraordinary transmission phenomenon through subwavelength hole arrays have been theoretically examined [3–9] and experimentally investigated [10–16]. It has been realized that the dimensions and periodicity of the holes in an array have a huge influence on the transmission spectrum. Surface plasmons compensate for the poor transmission figures through each hole. Every hole acts like a point source and the phenomenon can be described as a reconstruction of the incident beam at the exit side by means of a classical interference mechanism. On the other hand, a single aperture could be thought of as the simplest optical component. Therefore, the single aperture case was also considered in a similar treatment. Wave propagation through these single slits was analyzed [17–20]. Corrugations were added around the aperture in order to provide the necessary momentum and energy matching conditions. As a result, the transmission efficiency of the single aperture was significantly increased [21, 22]. The incoming wave was coupled to these periodic grooves that were located around the aperture and a narrow beam at the output side could be generated [23–27]. Moreover, such a simple device illustrates broad technological implications. The ability to concentrate the photons at a tiny aperture opens up technological possibilities and application fields. These application fields demand optical signals beyond the diffraction limit. Super-resolution is intended to be achieved by the use of subwavelength holes [28]. The aperture configurations were adapted to extract more light out of the system [29, 30]. Surface plasmon assisted lithography techniques that exploit the transmission enhancement methods were employed to attain smaller feature sizes [31, 32]. Further application fields include biophysics, chemical sensing, and molecular fluorescence [33–35]. Subwavelength apertures have been utilized in many ways and have proven to be promising candidates for scientific innovations.

Surface plasmons are not thought to exist in the microwave region. Nevertheless, subwavelength holes create spoof plasmons at microwave frequencies, and these spoof plasmons play the same role as their counterparts do in the optical domain [36, 37]. Plasmon-like waves govern the main physics, even though the metals are perfect conductors at these wavelengths. Additionally, metamaterials with their subwavelength features already have a well-established background in the microwave regime [38]. Hence, Alu *et al*. suggested covering the aperture with a metamaterial slab that would lead to improved transmission figures by minimizing the diffraction losses [39]. Independently, Marques *et al*. developed theories that discussed the analytical models of split ring resonators (SRRs) that were incorporated with an aperture [40]. Recently, Aydin *et al*. experimentally showed a 740-fold

#121693 - $15.00 USD Received 17 Dec 2009; revised 31 Jan 2010; accepted 2 Feb 2010; published 12 Feb 2010

transmission enhancement by guiding the incoming wave into the subwavelength aperture with the help of the metamaterials [41]. A SRR was used in order to effectively couple the electromagnetic waves to the output side. Aydin *et al*. worked with an aperture whose radius was 20 times smaller than the operational wavelength. Subsequently, Cakmak *et al*. discussed the physical origins of such an enhancement by considering a SRR that was excited by the electric field component of the incident beam at the SRR's resonance frequency [42]. Various other types of metamaterials were also combined with subwavelength apertures in later studies that yielded extraordinary transmission [43, 44]. However, in the present paper we present an approach that offers astonishingly higher transmission results while working with a super tiny aperture. We report these drastically improved transmission figures through a deep subwavelength aperture with an electrical effective area that is significantly smaller than the operational wavelength. Instead of employing electrically large covers or corrugations around the aperture [21–35, 39] to facilitate the input signal coupling, our approach makes use of the magnetic resonance of the connected SRRs (CSRRs) that are integrated with an electrically miniaturized hole at microwave frequencies. In the following sections of the present paper, we aim to address both the theoretical and experimental analysis of the transmission enhancement mechanism that is maintained by the aid of two types of CSRR configurations. We conclude by discussing the novelties that the CSRRs exhibit compared to the earlier studies that were also realized with the adjustment of single negative metamaterials around the subwavelength apertures.

2. CSRR designs and experimental setup

The respective design parameters of the CSRRs (Sample A&B) are depicted in Fig. 1(a). We have demonstrated the extraordinary transmission by using these samples. These distinct SRR samples are deposited on a dielectric printed circuit board (PCB). The PCBs are used in the experiments as a substrate layer with a thickness of 1.6mm. The deposited copper thickness is 30μm. The split width, g, is the same for the inner and outer rings in all configurations and is equal to 0.5mm. The same is true for the copper width, w, and its value is again 0.5mm for each case. The separation distance between the SRRs, l, is identical for both samples and is 5.5mm.

We simulated the transmission characteristics of these configurations in order to determine the magnetic resonance frequencies. These simulations were carried out in CST Microwave Studio. The same structures were realized in the simulation environment and the transmission results were collected as it is illustrated in Fig. 1(b). Periodic boundary conditions were adopted in the simulations. The structures were illuminated with an incident wave whose magnetic field component was perpendicular to the SRR plane, while the electric field component was along the SRRs' splits.

The respective magnetic resonance frequencies of the configurations are shown in Table 1. The resonance frequencies shift to relatively higher values for the combined systems. SRRs can be modeled with inductors and capacitors [40]. The two resonators having the same characteristics are merged. In the end, the resonance frequency is slightly altered due to the non-ideal contributions coming from the uncompensated inductors and capacitors of the overall system. Moreover, the resonance strength of the combined system is considerably reduced. It is reasonable to expect a drop in the resonance strength of the CSRRs since the split gaps are shorted as we join two SRRs together. We force the SRRs to work in phase with each other. The CSRRs may not be an intelligent choice as single negative metamaterials at these frequencies, but they are going to serve as a key element for our purposes during the transmission enhancement phenomenon. The details are discussed in the subsequent sections.

#121693 - $15.00 USD Received 17 Dec 2009; revised 31 Jan 2010; accepted 2 Feb 2010; published 12 Feb 2010

Table 1. List of the magnetic resonance frequencies

Configuration	f_{res}
Sample A	3.61 GHz
SRRA	3.53 GHz
Sample B	4.34 GHz
SRRB	4.26 GHz

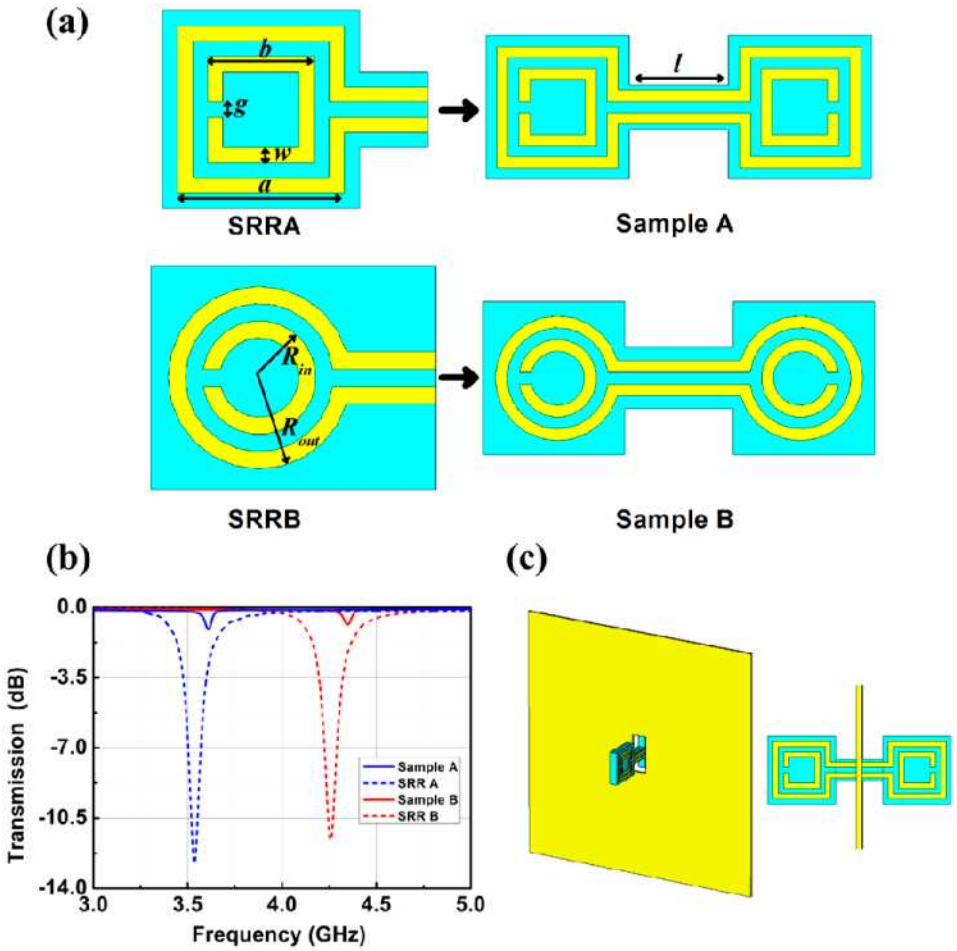

Fig. 1. (a) CSRR configurations and the labeled dimensions (a=5.5mm, b=3.5mm, g=w=0.5mm, l=5.5mm, R_{in}=1.75mm, R_{out}=3mm), (b) Simulated transmission spectra for Sample A (solid blue line), SRR A (dashed blue line), Sample B (solid red line), SRR B (dashed red line), and (c) Sample A incorporated with the deep subwavelength aperture. The front and side views are given together.

Figure 1(c) illustrates how we incorporate the samples with the aperture. We drilled an opening on a large metal plate of 1m×1m. The dimensions of the metal plate were intentionally picked to be large in order to minimize the diffraction effects at the edges. The thickness of the metal plate is 0.5mm. The opening on our metal screen constituted the subwavelength aperture. The area of the subwavelength aperture is $3\times7.5\text{mm}^2$ (width × height). The CSRRs are inserted inside the aperture. We tried to manually align the samples to

#121693 - $15.00 USD Received 17 Dec 2009; revised 31 Jan 2010; accepted 2 Feb 2010; published 12 Feb 2010

the midpoint of the aperture while leaving equal portions on both half planes. Transmission measurements were performed with conventional horn antennas operating around the frequency band of our interest. The antennas were located 8cm away from each other and the metal plate was positioned in between these antennas. The antennas were connected to the HP8510C Network Analyzer. The polarizations of the antennas were properly chosen to excite the magnetic resonance of the CSRR structure.

3. Results

3.1 Transmission results of the aperture

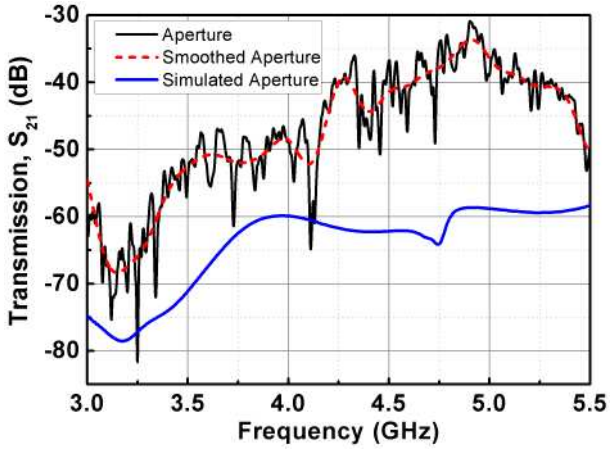

Fig. 2. Measured transmission results (solid black line), smoothed measurement results (dashed red line), simulated transmission results (solid blue line).

The transmission characteristics of the electrically large copper plate with the specified aperture were investigated. The numerical analyses are performed by modeling the horn antennas in CST Microwave Studio. The plate is inserted in between the antennas. The antennas are numerically characterized with their S parameters and radiation patterns. The modeled antennas have been validated to work in our frequency range with proper gain values and low losses. Then, the frequency response of the transmission through the aperture is collected both experimentally and numerically. S_{21}, which is defined as the ratio between the transmitted and the incident microwave signals in electrical engineering, is used as a measure of transmission in our examinations. Open boundary conditions were employed throughout the simulations in all directions. We tried to model the experimental setup in the simulation domain by staying loyal to the dimensions as much as possible. The simulated horn antennas were excited with waveguide ports. A dielectric constant ε=4 with a loss tangent of δ=0.014 was chosen to represent the dielectric media in our experiments. The copper had an electrical conductance of $\sigma_{cu}=5.8\times10^7$ S/m.

The simulation results are plotted in Fig. 2 (solid blue line). The transmission results are smaller than the actual signal to noise ratio of our Network Analyzer at certain frequencies. Such values would not be detectable in the experiments. Besides, simulations always offer better isolation and poor transmission figures. The diffractions at the edges of the metal plate are avoided in the simulations by placing perfect absorbers at the boundaries. Then, the transmission tends to increase as the frequency values get higher. However, the experiment results are not straightforward to process (solid black line). Sudden peaks and drops are caused by the higher order diffractions and reflections. The large plate is a perfect conductor at these frequencies and it deteriorates the measurement results by giving rise to the undesired scattered fields. It is rather difficult to simultaneously cancel those influences experimentally. Nonetheless, the transmission results of the aperture are going to be our references while acquiring the transmission enhancement results. We might end up with spurious enhancement

#121693 - $15.00 USD Received 17 Dec 2009; revised 31 Jan 2010; accepted 2 Feb 2010; published 12 Feb 2010

results (likely to be caused by the valleys) if we are not extra careful. In order to circumvent that possibility, we smoothed the measurement results to a reasonable level. The smoothed plot is also presented in Fig. 2 (dashed red line).

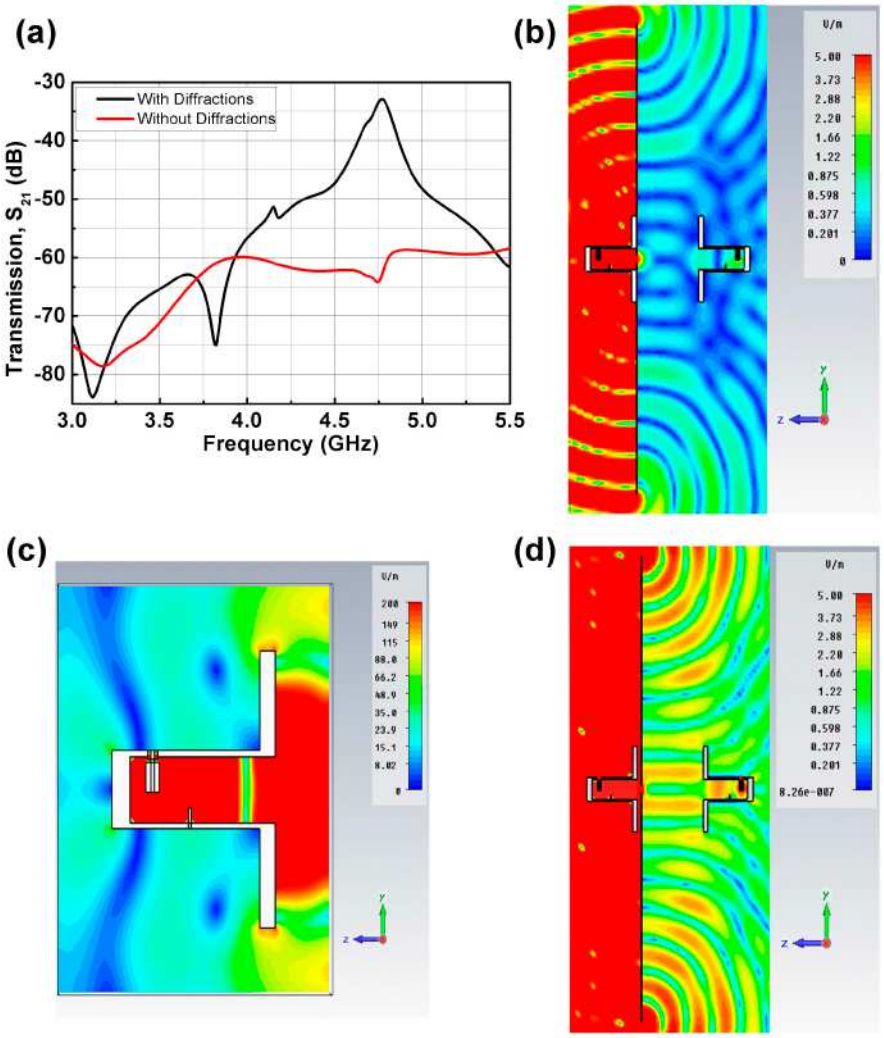

Fig. 3. (a) Simulated transmission results in the presence of diffractions (solid black line), and without diffractions (solid red line) when the transmitter antenna is 0.5mm away from the plate. (b) Simulated field maps on *y*-*z* plane when the transmitter antenna is 0.5mm away from the metal screen within a frequency range of 3.3-5 GHz (Media 1). (c) Simulated field maps on *y*-*z* plane for the modeled antennas within a frequency range of 3.5-5 GHz (Media 2). (d) Simulated field maps on *y*-*z* plane when the transmitter antenna is 5mm away from the metal screen within a frequency range of 3.3-5 GHz (Media 3).

We suspect that the transmission contributions of the diffraction mechanisms play an important role especially after 4 GHz. Diffractions are attributed to be the main difference in the absolute transmission values between the simulations and experiments. However, a further theoretical analysis is needed to clearly demonstrate their significance. The diffractions at the edges of the metal plate are taken into account while calculating the transmission coefficients in Fig. 3(a). The diffractions gave rise to almost 25 dB transmission improvement at higher frequencies and sudden drops start to appear in the transmission spectrum. Figure 3(b) illustrates the diffraction effects at the edges at 4.5 GHz. The transmitter antenna is placed

#121693 - $15.00 USD Received 17 Dec 2009; revised 31 Jan 2010; accepted 2 Feb 2010; published 12 Feb 2010

0.5mm away from the metal plate on the left hand side. The receiver antenna is aligned with the aperture and the transmitter antenna. It lies on the right hand side of Fig. 3(b). In this case, the diffracted fields act like a point source and an interference pattern is formed for different frequencies. This interference pattern explains the sudden peaks and drops in Fig. 2. The transmission through the subwavelength aperture is relatively weak in comparison to these diffraction effects. Still, in spite of the contributions coming from the diffractions, transmission results are lower than the experimental values. It is noteworthy fact that the fields can reach the edges even though the transmitter antenna is placed only 0.5mm apart from the subwavelength aperture. This can be best understood when we examine the mode profile at the exit of the waveguide portion of the horn antenna (see Fig. 3(c)). The fields rapidly extend in $\pm y$ directions. Then the separation distance between the transmitter antenna and the metal plate becomes the key parameter. The fields are plotted once again when we position the transmitter antenna 5mm away from the aperture (see Fig. 3(d)). The fields are depicted on the same scale. The diffraction clearly manifests itself and stronger interference patterns are observed at the receiver side. Subsequently, the discrepancies between the numerically attainable and experimentally collected single aperture transmission results are clarified. The transmission results for the single aperture turn out to be very sensitive to the variations in the separation distance between the plate and the transmitting horn antenna. We attempted to keep that distance as small as possible. However, it produces significant difficulties due to the mechanical limitations (e.g. the finite radius of curvature of the large and thin metal plate and the difficulty of the perfect manual alignment of the horn antenna with respect to the aperture).

3.2 Enhanced transmission results

The measured transmitted intensity results are portrayed in Fig. 4(a) and Fig. 4(d) in linear scale. The peaks are the evidence of the transmission enhancement in the presence of the samples. Single aperture transmission results were multiplied with 10 to be able to visualize both results on the same graph. Likewise, Fig. 4(b) and Fig. 4(e) depict the simulation results. The simulation results agree well with the experimental results. The enhancement peaks are spotted at similar frequencies. Finally, the measured enhancement figures are plotted in Fig. 4(c) and (f). The enhancement results are calculated by dividing the transmission values obtained from the apertures with the samples to the only aperture case for every frequency that in turn gives an estimate of the power gain of the overall system. The transmission enhancement took place at the respective frequencies that are listed in Table 2. At these frequencies, the subwavelength aperture is $\lambda/31\times\lambda/12$ (width × height) for Sample A, and $\lambda/25\times\lambda/10$ (width × height) for Sample B. We experimentally observed a more than 70,000 times power transmission enhancement for Sample A, whereas a higher than 5,300-fold power transmission improvement was achieved with Sample B. These values are much higher than the earlier reported results [41, 42]. Sample A generated an order of magnitude higher enhanced transmission figure. The main reason for this is that Sample A is designed to operate at lower frequencies, where the single aperture transmission is considerably lower (see Fig. 2).

Table 2. Transmission Enhancement

Configuration	f_{enh}	Subwavelength Aperture in terms of λ_{enh} (width × height)	Power Transmission Enhancement Figure
Sample A	3.23 GHz	$\lambda/31\times\lambda/12$	70,860
Sample B	4.03 GHz	$\lambda/25\times\lambda/10$	5,350

#121693 - $15.00 USD Received 17 Dec 2009; revised 31 Jan 2010; accepted 2 Feb 2010; published 12 Feb 2010

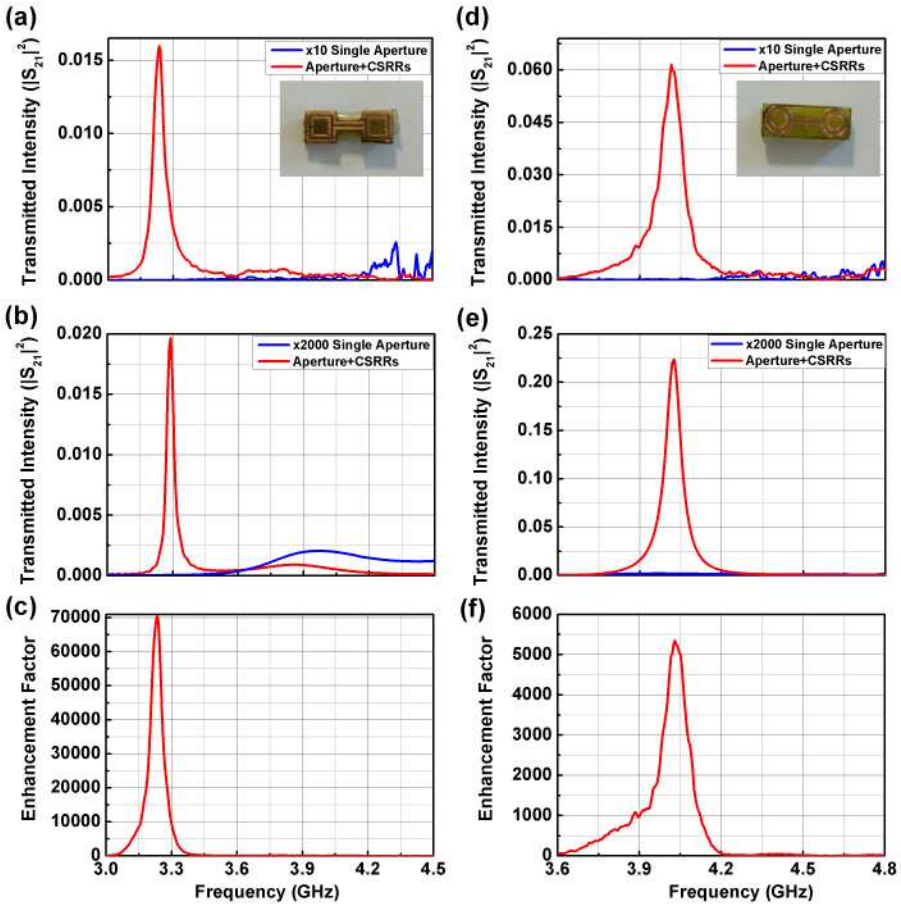

Fig. 4. (a) Measured, (b) simulated transmitted intensity results for Sample A (solid red lines) and the aperture (solid blue lines). (c) Experimentally validated enhancement factor for Sample A. (d) Measured, (e) simulated transmitted intensity results for Sample B (solid red lines) and the aperture (solid blue lines). (f) Experimentally validated enhancement factor for Sample B.

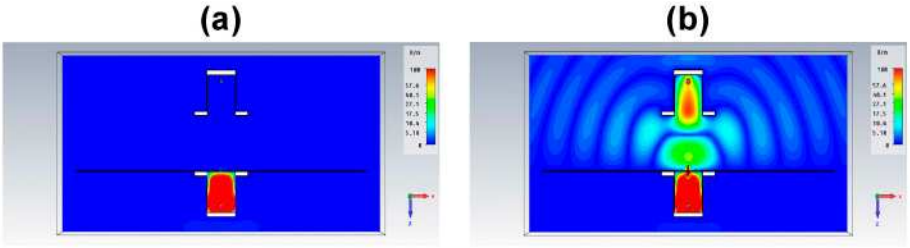

Fig. 5. Simulated field maps on *x*-*z* plane for (a) the single aperture case, (b) Sample A incorporated subwavelength aperture case at the numerically calculated enhancement frequency (3.3 GHz). The transmitter antenna is in the lower half plane and it is located 0.5mm away from the metal plate.

Figure 5 demonstrates the transmission enhancement phenomenon by making use of the field maps. The field maps are plotted on the same scale in order to exhibit the power coupling efficiency from the input side to the output side in the presence of the CSRRs. The simulated electric fields have no significant component that penetrated to the output side through the subwavelength hole for the single aperture case. Counter intuitively, the field magnitudes are drastically enhanced when we situate Sample A, another substance into the

#121693 - $15.00 USD Received 17 Dec 2009; revised 31 Jan 2010; accepted 2 Feb 2010; published 12 Feb 2010

electrically small aperture. The next section of the present study is devoted to the detailed physical discussions of this surprising phenomenon. Nevertheless, we can immediately state that CSRRs improve the transmission enhancement by thoroughly guiding the incident waves to the output side. Furthermore, the guided beams are focused to a certain point at the output side, which facilitates subwavelength focusing at the same time (see Fig. 5(b)).

It should also be noted that even higher enhancement factors are achievable numerically. Numerical analyses point out to a power transmission improvement of 800,000 and 225,000 for Sample A and Sample B respectively owing to the lower single aperture transmission figures. Consequently, several orders of higher transmission enhancement figures are theoretically available.

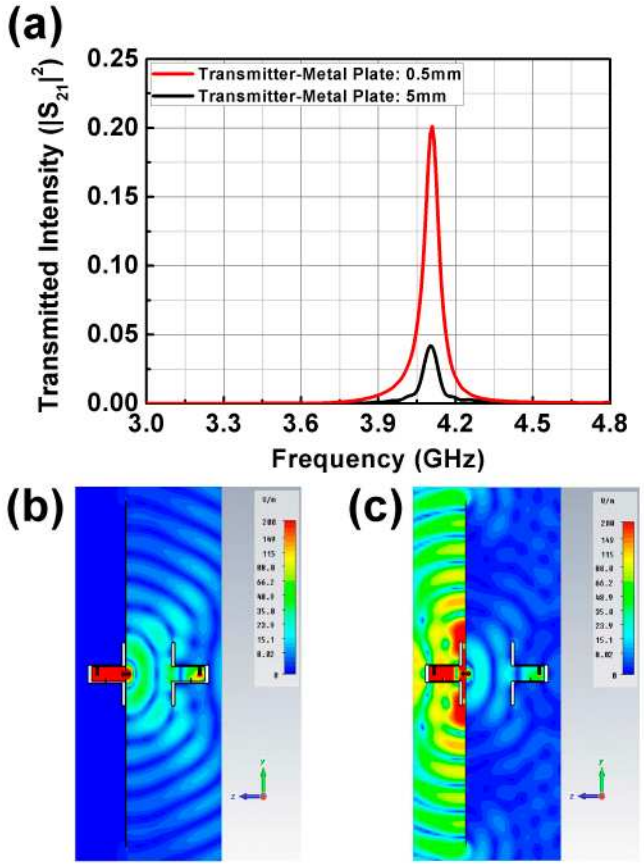

Fig. 6. (a) Simulated transmitted intensity figures for different transmitter antenna metal plate separations with Sample B (Metal plate-transmitter distance: 0.5mm solid red line, metal plate-transmitter distance: 5mm solid black line). Simulated field maps on *y*-*z* plane in the presence of Sample B when transmitter antenna to the metal plate separation is (b) 0.5mm and (c) 5mm.

The minor discrepancies in between the calculated and measured enhancement frequencies are associated with the small variations in the manufacturing processes, the crude modeling and insufficient meshing of the materials in the simulation domain as well as the possible slight misalignments in the experiments. Yet, the main differences in the absolute transmission values are again attributed to the diffraction effects as it is pointed out in Fig. 6. A significant portion of the incident beam is not properly coupled to the aperture but lost to the diffractions and scatterings instead. Hence, the absolute transmission value of the CSRR loaded aperture is also very sensitive to the separation distance especially after 4 GHz, where the diffractions within the system are more pronounced. The mechanical limitations compel

#121693 - $15.00 USD Received 17 Dec 2009; revised 31 Jan 2010; accepted 2 Feb 2010; published 12 Feb 2010

us to work with very precise positioners for the repeatability of the absolute transmission values that remain above 4 GHz throughout the experiments.

4. Understanding the transmission enhancement phenomenon

4.1 Simulation method

In the previous section, the horn antennas were modeled in order to investigate the transmission enhancement performances of the proposed samples realistically. A rather large real life electromagnetic problem was realized in the computational domain. Thus, we had the opportunity to compare the absolute transmission and transmission enhancement values within the operational frequency range of the horn antennas (3-5.5 GHz). Nonetheless, we need a broadband excitation source that can allow us to explore the deep subwavelength regime that covers frequencies even lower than 3 GHz. Therefore, we excite our structures with a plane wave in this section, which is dedicated to the understanding of the transmission enhancement phenomenon. The plane wave excitation enabled us to make a fair quantitative comparison between the enhancement figures appearing at distinct frequencies since the results are independent of the frequency response of the transmitting and receiving antennas. The electric field values are recorded by utilizing probes that were located 12.5cm away from the aperture. The boundary termination conditions were selected in such a way that the diffractions from the plate edges are totally obstructed.

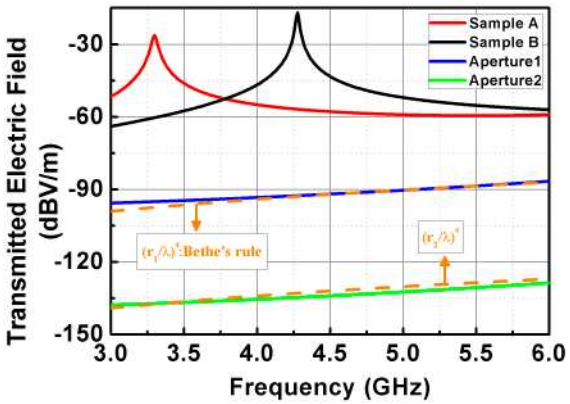

Fig. 7. Plane wave transmission results in dB scale collected with E-field probes for Sample A (solid red line), Sample B (solid black line), Aperture1 (solid blue line) and Aperture2 (solid green line). Bethe's transmission efficiency predictions for Aperture1 and Aperture2 (dashed orange lines).

Figure 7 shows the transmitted electric field values in dBV/m scale. Samples yielded a transmitted electric field improvement at around the expected frequencies. We worked with two different apertures. Aperture1 is $3\times7.5\text{mm}^2$ and Aperture2 is $1\times2.5\text{mm}^2$. On the other hand, Bethe's well-known transmission prediction for an annular hole on a two dimensional infinitely extending screen [1] is plotted in the same graph (dashed orange lines). It is apparent that Bethe's prediction provides a reliable insight. Bethe's predictions are adapted and fitted for the two apertures. The ratio of the fitting constants, r_1/r_2 is $(100)^{1/3} \approx 4.64$.

4.2 The role of magnetic resonance

The main reason for the transmission enhancement is the magnetic response of the SRRs. The incident fields are trapped inside the magnetic loop of the SRRs. The incoming waves are properly coupled to the aperture and guided to the output side. The transmission enhancement frequencies (see Table 2) are close to the calculated magnetic resonance frequencies of the samples (see Table 1), even though a periodic arrangement was simulated while identifying the transmission spectrum of the CSRRs. We tested the role of magnetic resonance in a canonical way by shorting the loops. We expect the transmission enhancement to disappear

#121693 - $15.00 USD Received 17 Dec 2009; revised 31 Jan 2010; accepted 2 Feb 2010; published 12 Feb 2010

when we short the loops. Figure 8 shows the simulated transmission and field enhancement results after we shorted the rings. Shorting the outer rings destroyed the magnetic resonance at around 4.2 GHz (solid blue line) and prevented the transmission enhancement for Sample B. Conversely, only the enhancement frequency is modified when the inner rings are shorted (solid black line). The magnetic response of the SRRs is not totally lost by solely shorting the inner rings. The outer rings still dominate the magnetic response within this frequency range. Hence, we can clearly state that the magnetic resonance is the responsible element for the transmission enhancement.

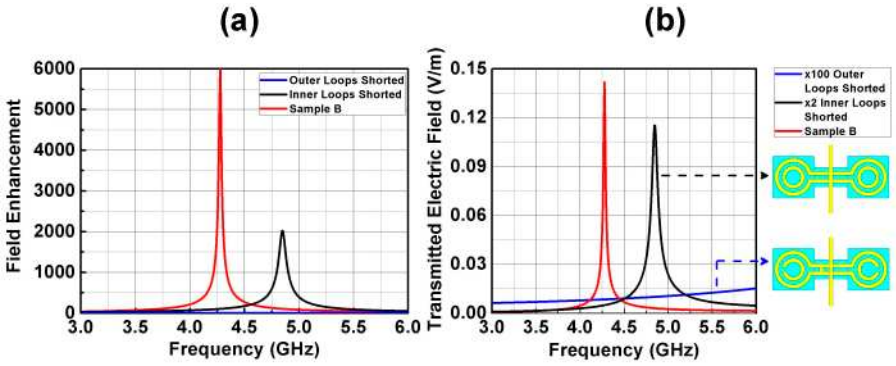

Fig. 8. (a) Simulated field enhancement results with respect to the single aperture for Sample B incorporated aperture (solid red line), Sample B with inner rings shorted (solid black line), and Sample B with outer rings shorted (solid blue line). (b) Simulated transmitted electric fields at the exit side for Sample B (solid red line), Sample B with inner rings shorted (solid black line), and Sample B with outer rings shorted (solid blue line).

4.2 The role of the aperture size and aperture independent transmission enhancement

Ref. 42 discusses the frequency blue shifts of the enhancement frequency with respect to the original magnetic resonance frequency. According to ref. 42, we have to treat the resonator together with the aperture as a combined system. Although the resonator establishes the grounds for a transmission enhancement, the two frequencies, namely the transmission enhancement frequency and the magnetic resonance frequencies of the samples do not match exactly. They are rather slightly separated. The slight mismatch between the magnetic resonance frequency values of the CSRRs (see Table 1) and the transmission enhancement frequencies of the respective CSRRs (see Table 2) are attributed to this effect. As the aperture shrinks, the enhancement frequency tends to move to higher frequencies.

The resonator sizes were always comparable to the subwavelength aperture size in previous studies [41–44]. Since the electromagnetic fields were highly localized around the aperture, the transmission enhancement frequencies were not highly robust against the changes in the geometrical parameters of the aperture. However, in the present study, we have a higher degree of freedom while designing the resonator structure. We do not have a strict restriction on the size of the resonator. Figure 9(b) shows the simulated transmission spectra for Aperture1 and Aperture2. The outer loop ring of the SRR has a width of 12.5mm, whereas the width of the inner rings is 10.5mm. Under these conditions, the selected resonator is significantly larger than the aperture. Nevertheless, the CSRRs still allow the incoming waves to interact with the aperture. Figure 9(b) demonstrates that the same amount of transmission is attained numerically regardless of the aperture size. Additionally, the amount of the transmitted fields through the aperture at these deep subwavelength frequencies is comparable to the previously obtained results for Sample B (see Fig. 8(b)). Consequently, tremendous field enhancement figures have been observed for an ultra-tiny aperture (in terms of its electrical size) in Fig. 9(a). This opens up the possibility for even more ambitious transmission enhancement results to be at least theoretically envisaged at these deep subwavelength frequencies. Furthermore, the transmission enhancement frequency has not

#121693 - $15.00 USD Received 17 Dec 2009; revised 31 Jan 2010; accepted 2 Feb 2010; published 12 Feb 2010

changed, owing to the aperture independent nature of the proposed transmission enhancement mechanism.

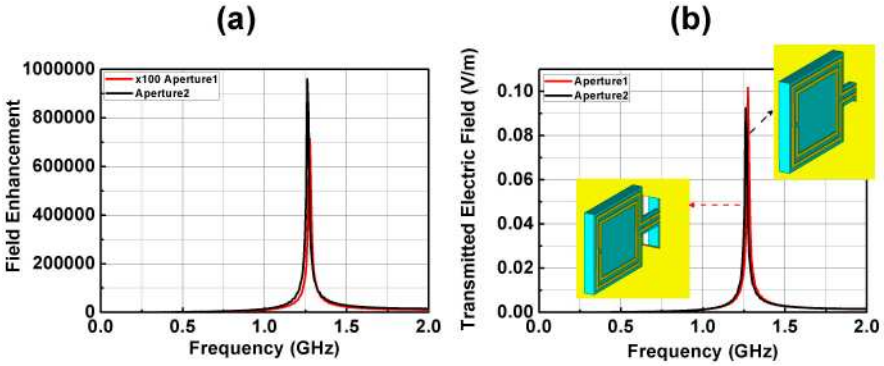

Fig. 9. (a) Simulated field enhancement results with respect to the single aperture for the CSRR with given dimensions. The same CSRR is incorporated with Aperture1 (solid red line), which is $3\times7.5\text{mm}^2$ and with Aperture2 (solid black line), which is $1\times2.5\text{mm}^2$. (b) Simulated transmitted electric fields at the exit side for Aperture1 (solid red line) and Aperture2 (solid black line).

4.3 The role of the connecting bars

The aperture independent transmission mechanism suggests clues for the role of the connecting bars. In the earlier studies [41–44], resonators were attached to one side of the metal plate. This case was investigated numerically, and the transmission characteristics are plotted in Fig. 10 (solid blue line). We omitted the SRR at the exit side of the aperture. Single SRR produced a relatively moderate transmission in accordance with the earlier reported results. Additionally, the transmission results without the connecting bars were checked in order to distinguish their role in the enhancement phenomenon. SRRs without the connecting bar provide better coupling compared to the single SRR case. However, Sample A still yields superior transmission, in turn resulting in amazingly higher enhancement figures. Moreover, the presence of the connecting bars once again manifests itself when we examine the shifts in the enhancement frequencies. Connecting bars brought aperture independency to the system, while keeping the enhancement resonance frequency close to the resonance frequency of the SRRs.

Several of these topics were addressed in Fig. 11. The magnetic response of the SRRs causes excess amounts of looping induced surface currents (see Fig. 11(a)). Only at the resonance frequency, the SRRs start working in phase by sharing equal portions of the induced surface currents. The incoming fields are trapped around the aperture due to this magnetic resonance, as shown in Fig. 11(b). Originally, the fields are concentrated and enhanced in the vicinity of the split width of the SRR that is located at the input side, as previously discussed in ref. 41. Once the fields are localized with the assistance of the SRR, the connected bars couple the waves by safely guiding them through the aperture. The second SRR at the output side is strongly excited (Fig. 11(d)) compared to the case without the connecting bars (Fig. 11(c)). Single SRR might be a better resonator. It might store stronger electrical fields, yet it lacks the ability to properly excite the second SRR. In our scheme, SRRs are not isolated any longer. The fields remain inside the loops. Individual SRRs stop working separately and the overall system acts like an antenna linking the input to the output. Trapped fields and induced surface currents are shared equally between the two resonators. Eventually, it provides an improved coupling mechanism between the input and output planes.

#121693 - $15.00 USD Received 17 Dec 2009; revised 31 Jan 2010; accepted 2 Feb 2010; published 12 Feb 2010

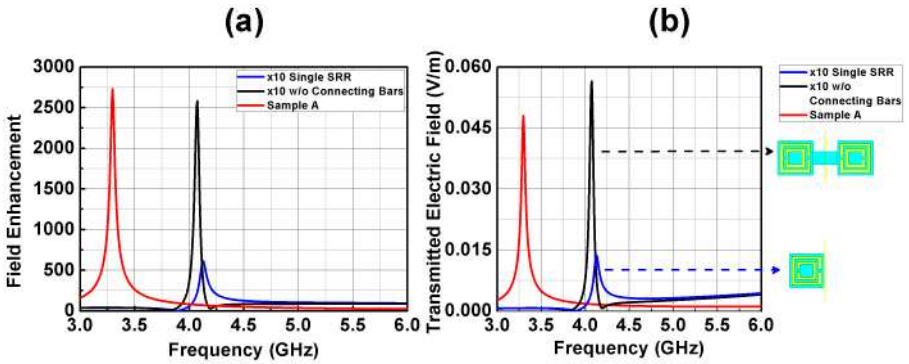

Fig. 10. (a) Simulated field enhancement results with respect to the single aperture for Sample A incorporated aperture (solid red line), Sample A without connecting bars (solid black line), and single SRR (solid blue line). (b) Simulated transmitted electric fields at the exit side for Sample A incorporated aperture (solid red line), Sample A without connecting bars (solid black line), and single SRR affixed to the input side of the aperture (solid blue line).

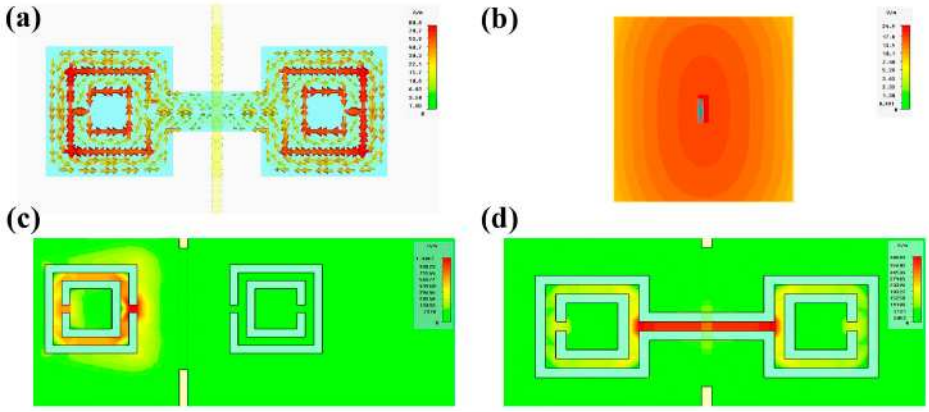

Fig. 11. Animations based on numerical results at the enhancement frequency. (a) Induced surface currents on the CSRRs (Media 4). (b) Field localization around the aperture (aperture is in the middle of the plane) with the help of the CSRRs (Media 5). (c) Electric field localization around the aperture without the connecting bars (Media 6). (d) Electric field localization around the aperture with the connecting bars (Media 7).

5. Conclusion

In summary, we presented an alternative approach that offers higher transmission enhancement results than the previously studied methods. We numerically simulated the transmission characteristics of a subwavelength aperture incorporated with the CSRRs. The transmission peaks that appeared in the simulation results suggested transmission enhancement. We also verified the transmission enhancement phenomenon experimentally. Our experiments indicated a transmission improvement factor above 70,000 through a subwavelength aperture that had a width of λ/31 and a height of λ/12 in terms of the operational wavelength. We discussed the diffraction mechanisms, mechanical difficulties and the key parameters of our experimental setup in order to achieve high transmission improvement results. We have shown that even higher transmission enhancement figures are numerically available. We attempted to emphasize the role of the connecting bars during this process. We numerically showed that the connecting bars linked the otherwise isolated SRRs to each other and guided the incoming wave through the subwavelength hole. The highly localized fields around the aperture, owing to the magnetic resonance of the SRRs, efficiently coupled the input wave to the exit side. This approach brings in the opportunity of attaining

#121693 - $15.00 USD Received 17 Dec 2009; revised 31 Jan 2010; accepted 2 Feb 2010; published 12 Feb 2010

excessive transmission enhancement factors by minimizing the dependence on the aperture geometry.

Electromagnetic transmission through a subwavelength hole used to be a challenging problem that belonged to the area of physics. However, researchers have tackled these difficulties by employing different kinds of coupling structures around the aperture in recent years. These innovations immediately found technological applications. The devices that relied on the extraordinary transmission effects were adopted in nanophotonics, biophysics, chemical sensing, nanolithography, and more. Yet, we analyzed the case with a single resonator that was located in the vicinity of a hole instead of the electrically large designs that have been made technologically available. We obtained very large transmission enhancement factors by making use of the CSRRs. A single resonator is easier to tune and control. We believe a device that is based on the CSRRs can be engineered in the optical domain. Such a device would enhance our resolution and signal strength, which might enable us to see how deep the rabbit hole goes.

Acknowledgements

This work is supported by the European Union under the projects EU-PHOME, and EU-ECONAM, and TUBITAK under Project Nos., 107A004, and 107A012. One of the authors (E.O.) also acknowledges partial support from the Turkish Academy of Sciences. Work at Ames Laboratory was supported by the Department of Energy Basic Energy Science under Contract No. DE-ACD2-07CH11358. The author (R.Z.) specially acknowledges the China Scholarship Council (CSC) for the financial support.

#121693 - $15.00 USD Received 17 Dec 2009; revised 31 Jan 2010; accepted 2 Feb 2010; published 12 Feb 2010